



Flanders
State of
the Art

18_153_1
FHR reports

iFlow-Inwerking en ontwikkeling SKN 21

Incorporation of intertidal zones in iFlow

DEPARTMENT
MOBILITY &
PUBLIC
WORKS

www.flandershydraulicsresearch.be

iFlow-Inwerking en ontwikkeling SKN 21

Incorporation of intertidal zones in iFlow

Kaptein, S.J.; Schramkowski, G.; Mostaert, F.

Legal notice

Flanders Hydraulics Research is of the opinion that the information and positions in this report are substantiated by the available data and knowledge at the time of writing.
The positions taken in this report are those of Flanders Hydraulics Research and do not reflect necessarily the opinion of the Government of Flanders or any of its institutions.
Flanders Hydraulics Research nor any person or company acting on behalf of Flanders Hydraulics Research is responsible for any loss or damage arising from the use of the information in this report.

Copyright and citation

© The Government of Flanders, Department of Mobility and Public Works, Flanders Hydraulics Research 2020
D/2020/3241/45

This publication should be cited as follows:

Kaptein, S.J.; Schramkowski, G.; Mostaert, F. (2020). iFlow-Inwerking en ontwikkeling SKN 21: Incorporation of intertidal zones in iFlow. Version 2.0. FHR Reports, 18_153_1. Flanders Hydraulics Research: Antwerp.

Reproduction of and reference to this publication is authorised provided the source is acknowledged correctly.

Document identification

| | | | |
|------------------|---|--|-----------------|
| Customer: | Flanders hydraulics Research | Ref.: | WL2020R18_153_1 |
| Keywords (3-5): | Idealized modelling, numerical simulations, Scheldt, intertidal zones | | |
| Text (p.): | 24 | Appendices (p.): | 3 |
| Confidentiality: | <input checked="" type="checkbox"/> No | <input checked="" type="checkbox"/> Available online | |

| | |
|------------|---------------|
| Author(s): | Kaptein, S.J. |
|------------|---------------|

Control

| | Name | Signature |
|-----------------|------------------|-----------|
| Reviser(s): | Schramkowski, G. | |
| Project leader: | Schramkowski, G. | |

Approval

| | | |
|-------------------|--------------|---|
| Head of Division: | Mostaert, F. | Getekend door: Frank Mostaert (Signature) Getekend op: 2020-03-15 21:09:31 +01:00 Reden: Ik keur dit document goed <i>Frank Mostaert</i> |
|-------------------|--------------|---|

Abstract

In this report, we present the effect of incorporating tidal zones in the idealized, width-based model iFlow. It appears that incorporating intertidal zones affects the hydrodynamics (i.e. water levels and flow velocities) via four different mechanisms. Each mechanism has been implemented in the two existing solvers of iFlow, the semi-analytical solver and the numerical solver. An additional solver, the full analytical solver, was created and is applicable to estuary models with a horizontal bottom and an exponentially converging width. It was found that the differences in results between these solvers where overall converging quadratically with increasing grid resolution, emphasizing correct implementation. However, one of the terms, does only converge linearly for a horizontal bottom. In the case of a more realistic bottom, quadratic convergence is still obtained for two of the four terms, while a third term only converges linearly and the fourth term does not converge with increasing grid resolution at all. Although these convergence discrepancies require some additional attention, the error between the terms stays less than 1% giving confidence into the implementation. Overall, the incorporation of intertidal zones was found to have a significant effect on the prediction of the M4 tide. The quantification of this effect has not been realized, mainly because the unrealistic bathymetry used did not allow for a significant analysis. The investigation of the quantitative effect of intertidal zones on the Scheldt is left for a follow up study.

fields of knowledge:

Idealized modelling, numerical simulations, Scheldt, intertidal zones

Contents

| | |
|---|-----|
| Abstract..... | III |
| List of Figures | VI |
| List of Tables | VII |
| 1 Introduction | 1 |
| 2 Reformulation of the equations including the effects of intertidal zones | 2 |
| 2.1 Governing equations | 2 |
| 2.2 Perturbation method and extension to the width and depth variables..... | 3 |
| 2.3 Parameterization of depth and width variations..... | 5 |
| 3 Analytical results | 6 |
| 3.1 Analytical formulation, general case | 6 |
| 3.2 Analytical formulation, steady component..... | 7 |
| 3.2.1 Depth return flow | 8 |
| 3.2.2 Width return flow | 8 |
| 3.3 Analytical formulation, M4 component, general case | 9 |
| 3.4 Analytical solution for a horizontal bottom and an exponential width variation | 10 |
| 3.4.1 Equations | 10 |
| 3.4.2 Homogeneous solution | 11 |
| 3.4.3 Particular solutions | 11 |
| 3.4.4 Total solution..... | 11 |
| 3.4.5 Individual forcing terms..... | 12 |
| 4 Simulation results | 15 |
| 4.1 Validation..... | 15 |
| 4.2 Effect of the incorporation of intertidal zones on the total M4 surface elevation (horizontal bottom) | 20 |
| 4.3 Case of a varying bottom | 22 |
| 4.4 Conclusion..... | 23 |
| A1 Intermediate steps for the computation of the width/depth dependent M4 | A1 |
| A1.1 Resolution method for the particular solution | A1 |
| A1.2 Integration constants of the homogeneous solution | A2 |
| A1.3 Derivatives of the leading order solutions | A3 |

List of Figures

| | | |
|----------|---|----|
| Figure 1 | Evolution of the relative variation in width over the length of the estuary..... | 1 |
| Figure 2 | Evolution of the differences in water levels computed by the semi-analytical and the fully analytical solver (configuration of Wei <i>et al.</i> , 2016). | 16 |
| Figure 3 | Evolution of the differences in water levels computed by the numerical and the fully analytical solver (configuration of Wei <i>et al.</i> , 2016). | 17 |
| Figure 4 | Evolution of the differences in water levels computed by the numerical and the semi-analytical solver (configuration of Wei <i>et al.</i> , 2016). | 18 |
| Figure 5 | Evolution of the differences in water levels computed by the numerical and the fully analytical solver (configuration of Wei <i>et al.</i> , 2016). | 19 |
| Figure 6 | Leading order solutions for the water level and the bottom velocity for the Wei <i>et al.</i> , 2016 configuration. | 20 |
| Figure 7 | Leading order solutions for the water level and the bottom velocity for the Brouwer <i>et al.</i> , 2017 configuration. | 21 |
| Figure 8 | First order surface elevation decomposed into separate width-depth contributions (Wei <i>et al.</i> , 2016) (only full analytical results). | 21 |
| Figure 9 | First order surface elevation decomposed into separate width-depth contributions (Wei <i>et al.</i> , 2016) (only full analytical results). | 22 |

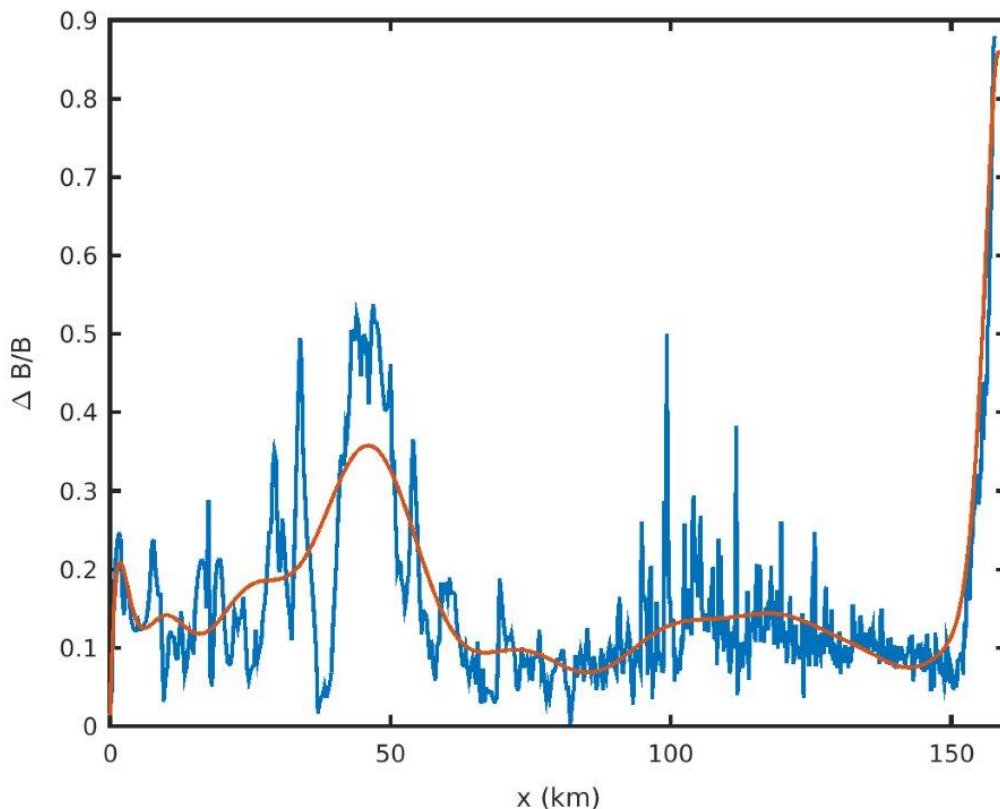
List of Tables

| | | |
|---------|--|----|
| Table 1 | Parameter values for an idealized Scheldt model (Wei <i>et al.</i> , 2016). | 15 |
| Table 2 | Parameter values for a different idealized Scheldt model Brouwer <i>et al.</i> , 2017. Note that these parameters also include a phase shift of -1.3° between the external M4 and the external M2 tides. | 20 |
| Table 3 | Coefficients for the polynomial approximation of the water depth..... | 22 |

1 Introduction

Processed based, exploratory models such as iFlow (Dijkstra *et al.*, 2017) have been used with increasing frequency over the last years, both in scientific research (Brouwer *et al.*, 2018; Dijkstra *et al.*, 2019a,b) or in studies following requests from customers (Brouwer *et al.*, 2017). The benefits of these models with respect to classical three-dimensional models (such as Telemac), is (i) their speed and (ii) the possibility to decompose output variables (e.g. water-level or flow velocity) into individual components related to specific physical mechanisms. A disadvantage of these models is that they are highly idealized or simplified in terms of both geometry and governing equations. This implies that some crucial mechanisms influencing the hydrodynamics or sediment transport might be overlooked. Since iFlow is a width-averaged model, the width of an estuary, as defined in the model, might vary over its length, but is always taken constant in time. Nevertheless, basic studies of bathymetry in the Scheldt show that the width of the Scheldt can vary with up to 40% on an intertidal time-scale at some location (see Fig. 1). This phenomenon is caused by large areas called intertidal zones, that are covered by water at high tide but fall dry during low-tide. This feature implies that some major properties of

Figure 1 – Evolution of the relative variation in width over the length of the estuary.



intertidal zones are not yet included in iFlow. An example of such a property is the additional volume offered by intertidal zones for storage of water, which has a direct impact on the water-level. A possibility to circumvent this shortcoming within the iFlow framework, is to modify its governing equations to allow the width of the estuary to vary with the water-level. In the remaining part of the report, we first discuss the adaptation of the governing equations. Subsequently, we evaluate our approach via the investigation of the parameter space for a simplified geometry of an estuary and compare analytical solutions to the iFlow results. Finally, the model with intertidal zone effects is applied to a realistic geometry of the Scheldt river.

2 Reformulation of the equations including the effects of intertidal zones

2.1 Governing equations

According to Dijkstra *et al.*, 2017, the governing equations in iFlow consist of a width-averaged Shallow-water equation for the conservation of momentum and two continuity equations. However, in the present study the vertical velocity does not play a role of interest. As a result, we limit ourselves to a width-averaged and depth-integrated equation for the conservation of mass governing the surface elevation. The equations of interest are

$$\frac{\partial u}{\partial t} + u \frac{\partial u}{\partial x} + w \frac{\partial u}{\partial z} = -g \frac{\partial \zeta}{\partial x} - \int_z^{R+\zeta} \frac{1}{\rho_{\text{ref}}} \frac{\partial \rho}{\partial x} d\tilde{z} + \frac{\partial}{\partial z} \left(\nu_T \frac{\partial u}{\partial z} \right), \quad (1a)$$

$$B \frac{\partial \zeta}{\partial t} + \frac{\partial}{\partial x} \left(B \int_{-H}^{R+\zeta} u dz \right) = 0 \quad (1b)$$

in which u is the horizontal velocity variable, ζ the surface elevation, x is the along estuary coordinate, z the vertical coordinate and t time. The symbol represents g the acceleration of gravity, R the mean level of the river surface, ρ_{ref} the reference density, ρ the density of the fluid, ν_T the eddy-viscosity, H the depth and B the width. It was chosen to highlight the width with a different color such that its role within the governing equations is more visible. The depth is also displayed in a different color because it is demonstrated in the Sec. 2.3 that width and depth are intrinsically linked via the width-averaging process.

A set of boundary conditions is associated to the governing equations. These boundary conditions comprise a partial slip condition at the bed (i.e. $z = -H$), a no-stress condition at the surface (i.e. $z = R + \zeta$), a time-dependent tidal forcing at the seaward boundary (i.e. $x = 0$) and an imposed river discharge at the landward boundary (i.e. $x = L$). The equations for these boundary conditions are

$$\nu_T \frac{\partial u}{\partial z} = s_f u \quad \text{at } z = -H, \quad (2a)$$

$$\nu_T \frac{\partial u}{\partial z} = 0 \quad \text{at } z = R + \zeta, \quad (2b)$$

$$\zeta = A_{M_2} \cos(\sigma t) + A_{M_4} \cos(2\sigma t + \varphi) \quad \text{at } x = 0, \quad (2c)$$

$$B \int_{-H}^{R+\zeta} u dz = -Q \quad \text{at } x = L, \quad (2d)$$

respectively. Several parameters appear: s_f , the friction coefficient, A_{M_2} and σ , respectively the amplitude and the frequency of the M_2 tide, and A_{M_4} , the amplitude of the M_4 tide.

2.2 Perturbation method and extension to the width and depth variables

The iFlow philosophy for solving the governing equations is based on the perturbation technique. The first assumption upon which this technique is based is that some of the variables are decomposable into a series of terms. In these series, each term is of order $\varepsilon = \zeta/H$ with respect to the previous term and $\varepsilon \ll 1$. For example, a variable η can be written as

$$\eta = \eta_0 + \eta_1 + \eta_2 + \dots$$

with $\eta_1/\eta_0 = O(\varepsilon)$, $\eta_2/\eta_1 = O(\varepsilon)$, etc. Up to now, this decomposition technique has been applied to the unknown variables (i.e. u , w and ζ), as well as to some of the physical mechanisms (tidal elevation at the seaward boundary, river flux at the landward boundary), but not to the width B or to the depth H . From now on, also these variables are split following

$$\begin{aligned} B &= B_0 + B_1 + \dots, \\ H &= H_0 + H_1 + \dots. \end{aligned}$$

The second assumption of the perturbation technique is based on a harmonic decomposition. The harmonic decomposition implies that each variable evolves periodically in time, according to a specific frequency that is characteristic of the variable's order. At leading order, the variables will evolve according to the frequency of the M2 tide, while at first order, the variables will evolve according to the frequency of the M4 tide, but will also have a time-independent component referred to as the 'M0 frequency'. As a result of this assumption, it is very useful to define a complex function, denoted by $\hat{\cdot}$, verifying

$$\eta_0(x, z, t) = \frac{\hat{\eta}_{02}(x, z)}{2} e^{i\sigma t} + \frac{\hat{\eta}_{02}^*(x, z)}{2} e^{-i\sigma t} \quad (3)$$

$$\eta_1(x, z, t) = \underbrace{\frac{\hat{\eta}_{14}(x, z)}{2} e^{2i\sigma t} + \frac{\hat{\eta}_{14}^*(x, z)}{2} e^{-2i\sigma t}}_{\eta_{14}} + \eta_{10} \quad (4)$$

where η designates either u , w or ζ . The first order solution consist of a signal evolving as $2\sigma t$, which has a complex amplitude of $|\hat{\eta}_{14}|$, and a time-independent signal, of amplitude η_{10} . In these notations, the first subscript (hereafter also denoted p) refers to the order and the second subscript (hereafter also denoted k) refers to the tidal component. The superscript * denotes the complex conjugated associated to $\hat{\eta}$. By defining $\hat{\eta}_{pk} = |\hat{\eta}_{pk}| e^{i\varphi}$, it is then easy to show that

$$\eta_0 = |\hat{\eta}_{02}(x, z)| \cos(\sigma t + \varphi(x, z)), \quad (5)$$

$$\eta_{14} = |\hat{\eta}_{14}(x, z)| \cos(2\sigma t + \varphi(x, z)), \quad (6)$$

in other words, the amplitudes of η_{pk} and $\hat{\eta}_{pk}$ are equal. This formulation has implications for the time derivatives

$$\frac{\partial \hat{f}_n}{\partial t} = ni\sigma \hat{f}_n.$$

This second assumption directly implies that the parameterization of B and H has be chosen such that the velocity and flow patterns they generate are consistent with Eqs (3) and (4). This condition will be further detailed in Sec. 2.3.

Applying the decomposition method to the set of governing equations Eqs.(1a-??) gives at leading order

$$\frac{\partial u_0}{\partial t} - \frac{\partial}{\partial z} \left(\nu_x \frac{\partial u_0}{\partial z} \right) = -g \frac{\partial \zeta_0}{\partial x}, \quad (7a)$$

$$B_0 \frac{\partial \zeta_0}{\partial t} + \frac{\partial}{\partial x} \left(B_0 \int_{-H_0}^R u_0 dz \right) = 0, \quad (7b)$$

for the governing equations, and

$$\nu_T \frac{\partial u_0}{\partial z} = s_f u_0 \quad \text{at } z = -H_0, \quad (8a)$$

$$\nu_T \frac{\partial u_0}{\partial z} = 0 \quad \text{at } z = R, \quad (8b)$$

$$\zeta_0 = A_{M_2} \cos(\sigma t) \quad \text{at } x = 0, \quad (8c)$$

$$B_0 \int_{-H_0}^R u_0 dz = 0 \quad \text{at } x = L, \quad (8d)$$

for the boundary conditions. For the exact scaling assumptions, in particular for the convective terms and the baroclinic term, the reader is referred to Chernetsky *et al.*, 2010; Dijkstra *et al.*, 2017. The attentive reader will remark that at leading order no changes have occurred to the governing equations, which is in agreement with the hypothesis that width variations only appear at first order.

At first order, the governing equations Eqs.(1a-1b) become

$$\frac{\partial u_1}{\partial t} - \frac{\partial}{\partial z} \left(\nu_T \frac{\partial u_1}{\partial z} \right) = -g \frac{\partial \zeta_1}{\partial x} - \int_z^R \frac{1}{\rho_{\text{ref}}} \frac{\partial \rho_0}{\partial x} dz - u_0 \frac{\partial u_0}{\partial x} - w_0 \frac{\partial u_0}{\partial z}, \quad (9a)$$

$$B_0 \frac{\partial \zeta_1}{\partial t} = - \frac{\partial}{\partial x} \left(B_0 \int_{-H_0}^R u_1 dz \right) - \frac{\partial}{\partial x} (B_0 u_0|_R \zeta_0) - \frac{\partial}{\partial x} (B_0 u_0|_{-H_0} H_1) - B_1 \frac{\partial \zeta_0}{\partial t} - \frac{\partial}{\partial x} \left(B_1 \int_{-H_0}^R u_0 dz \right), \quad (9b)$$

Additional depth forcing
Additional width forcing

for the governing equations, and

$$\nu_T \frac{\partial u_1}{\partial z} = s_f u_1 - \underbrace{s_f H_1 \frac{\partial u_0}{\partial z} + H_1 \frac{\partial}{\partial z} \left(\nu_T \frac{\partial u_0}{\partial z} \right)}_{\text{Additional depth forcing}} \quad \text{at } z = -H_0, \quad (10a)$$

$$\nu_T \frac{\partial u_1}{\partial z} = -\zeta_0 \frac{\partial}{\partial z} \left(\nu_T \frac{\partial u_0}{\partial z} \right) \quad \text{at } z = R, \quad (10b)$$

$$\zeta_1 = A_{M_4} \cos(2\sigma t - \varphi) \quad \text{at } x = 0, \quad (10c)$$

$$\int_{-H_0}^R u_1 dz = -\frac{Q_1}{B_0} - u_0|_R \zeta_0 - \underbrace{u_0|_{-H_0} H_1}_{\text{Additional depth forcing}} - \underbrace{\frac{B_1}{B_0} \int_{-H_0}^R u_0 dz}_{\text{Additional width forcing}} \quad \text{at } x = L, \quad (10d)$$

for the boundary conditions. It is only at the first order that the width variations start to influence the equations of motion through the appearance of new forcing terms denoted 'additional width forcing' or 'additional depth forcing'. These two terms appear in the two continuity equations, in the bottom boundary condition and in the landward boundary condition, where the river flow rate is imposed.

2.3 Parameterization of depth and width variations

As mentioned previously, the parameterization of depth and width variation cannot be taken arbitrarily. In order to be consistent with the ordering and harmonic decomposition of the variables, it is required that B_0 and H_0 are constant, while B_1 and H_1 vary linearly with the water level ζ_{02} , the latter evolving with a σ -frequency. A parameterization satisfying these conditions for B is

$$B = B_0 + \underbrace{\frac{\Delta B}{2A_{M_2}}}_{B_1} \zeta_{02} + \dots, \quad (11)$$

where ΔB is the difference in width of the estuary between high and low water.

Since iFlow is a width-averaged model, conservation of the cross-section implies that changes in the estuary width also involve changes in the estuary depth. This implication is taken account for by defining variation of the cross-section \mathcal{A} with respect to the water depth as

$$\mathcal{A} = \int_{-\infty}^{\zeta} B(\zeta') d\zeta'. \quad (12)$$

Simultaneously, by definition

$$\mathcal{A} = B(\zeta) (H + \zeta). \quad (13)$$

Differentiation Eqs (12) and (13) against ζ , and equating the result gives

$$B(\zeta) = \frac{\partial B}{\partial \zeta} (H + \zeta) + B \frac{\partial H}{\partial \zeta} + B(\zeta). \quad (14)$$

Finally, by noticing that $H \gg \zeta$, a first order approximation gives

$$\frac{\partial H}{\partial \zeta} = -\frac{H}{B} \frac{\partial B}{\partial \zeta}. \quad (15)$$

Using Eq. (11) into Eq. (15) gives an ordering of H :

$$H(\zeta) = H_0 - \underbrace{\frac{H_0}{B_0} \frac{\Delta B}{2A_{M_2}}}_{H_1} \zeta_{02} \quad (16)$$

3 Analytical results

3.1 Analytical formulation, general case

The new terms related to width (and depth) variations only appear at first order. Accordingly, the resolution will focus on the equations for the first order variables. Equations (9a-9b) can be re-written introducing new symbols for the forcing terms in order to highlight them. For simplicity, the horizontal density gradient and the eddy viscosity are assumed to be constant over the vertical and the river elevation is neglected ($R = 0$). These assumptions give

$$\frac{\partial u_1}{\partial t} - \nu_T \frac{\partial^2 u_1}{\partial z^2} = -g \frac{\partial \zeta_1}{\partial x} - \xi(x, z, t) + g \left\langle \frac{\partial \rho}{\partial x} \right\rangle z, \quad (17a)$$

$$\frac{\partial \zeta_1}{\partial t} = - \left(\frac{\partial}{\partial x} + \frac{1}{B_0} \frac{\partial B_0}{\partial x} \right) \left(\int_{-H_0}^0 u_1 dz + \gamma^R(x, t) + \gamma^H(x, t) \right) - \frac{1}{B_0} \frac{\partial}{\partial x} \gamma^B(x, t) - \zeta^B(x, t), \quad (17b)$$

The associated boundary conditions, Eqs (10a-10d), can be simplified to

$$\frac{\partial u_1}{\partial z} = \frac{s_f}{\nu_T} u_1 + \chi^H(x, t) \quad \text{at } z = -H_0, \quad (18a)$$

$$\frac{\partial u_1}{\partial z} = -\chi^R(x, t) \quad \text{at } z = 0, \quad (18b)$$

$$\zeta_1 = A_{M_4} \cos(2\sigma t + \varphi) \quad \text{at } x = 0, \quad (18c)$$

$$\int_{-H_0}^0 u_1 dz = -\frac{Q_1}{B_0} - \gamma^R(x, t) - \gamma^H(x, t) - \frac{1}{B_0} \gamma^B(x, t) \quad \text{at } x = L. \quad (18d)$$

The newly introduced symbols, ξ , γ^R , γ^H , ζ^B , χ^R , χ^H and yield

$$\xi(x, z, t) = u_0(x, z, t) \frac{\partial u_0}{\partial x} + w_0(x, z, t) \frac{\partial u_0}{\partial z}, \quad (19a)$$

$$\gamma^R(x, t) = \zeta_0(x, t) u_0(x, t) \Big|_{z=0}, \quad (19b)$$

$$\gamma^H(x, t) = H_1(x, t) u_0(x, t) \Big|_{z=-H_0}, \quad (19c)$$

$$\gamma^B(x, t) = B_1 \int_{-H_0}^0 u_0 dz, \quad (19d)$$

$$\zeta^B(x, t) = \frac{B_1}{B_0} \frac{\partial \zeta_0}{\partial t}, \quad (19e)$$

$$\chi^H(x, t) = -\frac{s_f}{\nu_T} H_1 \frac{\partial u_0}{\partial z} \Big|_{-H_0} + H_1 \frac{\partial^2 u_0}{\partial z^2} \Big|_{-H_0}, \quad (19f)$$

$$\chi^R(x, t) = \zeta_0 \frac{\partial^2 u_0}{\partial z^2} \Big|_0, \quad (19g)$$

$$(19h)$$

3.2 Analytical formulation, steady component

Since the equations governing the steady state variables are linear, the solution consists of the sum of the solutions to the individual forcing terms. As a result, the forcing terms that are not related to width or depth variations will not be considered here. The equations governing the steady state component of the variables are obtained by replacing the different complex quantities by the formulation of Eqs (3), (4), which gives

$$\nu_T \frac{\partial^2 u_{10}}{\partial z^2} = g \frac{\partial \zeta_{10}}{\partial x}, \quad (20a)$$

$$0 = - \frac{\partial}{\partial x} \left(B_0 \left(\int_{-H_0}^0 u_{10} dz + \gamma_{10}^H(x) \right) + \gamma_{10}^B(x) \right) \quad (20b)$$

and the associated boundary conditions

$$\frac{\partial u_{10}}{\partial z} = \frac{s_f}{\nu_T} u_{10} + \chi_{10}^H(x) \quad \text{at } z = -H_0, \quad (21a)$$

$$\frac{\partial u_{10}}{\partial z} = 0 \quad \text{at } z = 0, \quad (21b)$$

$$\zeta_{10} = 0 \quad \text{at } x = 0, \quad (21c)$$

$$\int_{-H_0}^0 u_{10} dz = - \gamma_{10}^H(x) - \frac{1}{B_0} \gamma_{10}^B(x) \quad \text{at } x = L.. \quad (21d)$$

In these equations, the forcing terms of the steady state variables area

$$\gamma_{10}^H = \frac{\hat{H}_{12} \hat{u}_{02}^* + \hat{H}_{12}^* \hat{u}_{02}}{4}, \quad (22)$$

$$\gamma_{10}^B = \frac{1}{4} \hat{B}_{12} \int_{-H_0}^0 \hat{u}_{02}^* dx + \frac{1}{4} \hat{B}_{12}^* \int_{-H_0}^0 \hat{u}_{02} dx, \quad (23)$$

$$\chi_{10}^H = - \frac{1}{4} \frac{s_f}{\nu_T} \hat{H}_{12} \left. \frac{\partial \hat{u}_{02}^*}{\partial z} \right|_{-H_0} - \frac{1}{4} \frac{s_f}{\nu_T} \hat{H}_{12}^* \left. \frac{\partial \hat{u}_{02}}{\partial z} \right|_{-H_0} + \frac{1}{4} \hat{H}_{12} \left. \frac{\partial^2 \hat{u}_{02}^*}{\partial z^2} \right|_{-H_0} + \frac{1}{4} \hat{H}_{12}^* \left. \frac{\partial^2 \hat{u}_{02}}{\partial z^2} \right|_{-H_0}. \quad (24)$$

Additionally, integrating Eq. (20b) along x between x and L , using Eq. (21d) gives

$$\int_{-H_0}^0 u_{10} dz + \gamma_{10}^H(x) + \frac{1}{B_0} \gamma_{10}^B(x) = 0 \quad (25)$$

Depth induced partial slip The depth induced partial slip boundary condition velocity verifies

$$\frac{\partial^2 u_{\text{dips}}}{\partial z^2} = \frac{g}{\nu_T} \frac{\partial \zeta_{\text{dips}}}{\partial x}, \quad (26a)$$

$$\frac{\partial u_{\text{dips}}}{\partial z} = \frac{s_f}{\nu_T} u_{\text{dips}} + \chi_{10}^H(x) \quad \text{at } z = -H_0, \quad (26b)$$

$$\frac{\partial u_{\text{dips}}}{\partial z} = 0 \quad \text{at } z = 0. \quad (26c)$$

The solution to this set of equations is

$$u_{\text{dips}} = \left(\frac{z^2}{2\nu_T} - \frac{H_0^2}{2\nu_T} - \frac{H_0}{s_f} \right) g \frac{\partial \zeta_{\text{dips}}}{\partial x} - \frac{\nu_T}{s_f} \chi_{10}^H(x) \quad (27)$$

From Eq. (25), we have that

$$\int_{-H_0}^0 u_{\text{dips}} dz = 0, \quad (28)$$

so that

$$\frac{\partial \zeta_{\text{dips}}}{\partial x} = -\frac{H_0}{s_f} \frac{\nu_T}{g \left(\frac{1}{3} \frac{H_0^3}{\nu_T} + \frac{H_0^2}{s_f} \right)} \chi_{10}^H(x) \quad (29)$$

3.2.1 Depth return flow

The depth return flow velocity verifies

$$\frac{\partial^2 u_{\text{depth}}}{\partial z^2} = \frac{g}{\nu_T} \frac{\partial \zeta_{\text{depth}}}{\partial x}, \quad (30a)$$

$$\frac{\partial u_{\text{depth}}}{\partial z} = \frac{s_f}{\nu_T} u_{\text{depth}} \quad \text{at } z = -H_0, \quad (30b)$$

$$\frac{\partial u_{\text{depth}}}{\partial z} = 0 \quad \text{at } z = 0, \quad (30c)$$

$$(30d)$$

The solution to this set of equations is

$$u_{\text{depth}}(z) = \left(\frac{z^2}{2\nu_T} - \frac{H_0^2}{2\nu_T} - \frac{H_0}{s_f} \right) g \frac{\partial \zeta_{\text{depth}}}{\partial x}. \quad (31)$$

The depth return flow induced surface elevation follow from the condition

$$\int_{-H_0}^0 u_{\text{depth}} dz = -\gamma_{10}^H(x) \quad (32)$$

such that

$$\frac{\partial \zeta_{\text{depth}}}{\partial x} = \frac{\gamma_{10}^H(x)}{g \left(\frac{1}{3} \frac{H_0^3}{\nu_T} + \frac{H_0^2}{\nu_T} \right)} \quad (33)$$

3.2.2 Width return flow

The width return flow velocity verifies

$$\frac{\partial^2 u_{\text{width}}}{\partial z^2} = \frac{g}{\nu_T} \frac{\partial \zeta_{\text{width}}}{\partial x}, \quad (34a)$$

$$\frac{\partial u_{\text{width}}}{\partial z} = \frac{s_f}{\nu_T} u_{\text{width}} \quad \text{at } z = -H_0, \quad (34b)$$

$$\frac{\partial u_{\text{width}}}{\partial z} = 0 \quad \text{at } z = 0, \quad (34c)$$

$$(34d)$$

The solution to this set of equations is

$$u_{\text{width}}(z) = \left(\frac{z^2}{2\nu_T} - \frac{H_0^2}{2\nu_T} - \frac{H_0}{s_f} \right) g \frac{\partial \zeta_{\text{width}}}{\partial x}. \quad (35)$$

The width return flow induced surface elevation is given by

$$\int_{-H_0}^0 u_{\text{width}} dz = -\frac{1}{B_0} \gamma_{10}^B(x) \quad (36)$$

such that

$$\frac{\partial \zeta_{\text{width}}}{\partial x} = \frac{\gamma_{10}^B(x)}{g B_0 \left(\frac{1}{3} \frac{H_0^3}{\nu_T} + \frac{H_0^2}{\nu_T} \right)} \quad (37)$$

3.3 Analytical formulation, M4 component, general case

To find the equations governing the M4 tidal component, Eqs (4) and (3) are injected into the governing equations Eqs (17a) and (17b), and the associated boundary conditions (18a), (18b-18d), and projected on $e^{2i\sigma t}$.

$$2i\sigma \hat{u}_{14} - \nu_T \frac{\partial^2 \hat{u}_{14}}{\partial z^2} = -g \frac{\partial \hat{\zeta}_{14}}{\partial x} \quad (38a)$$

$$2i\sigma \hat{\zeta}_{14} = - \left(\frac{\partial}{\partial x} + \frac{1}{B_0} \frac{\partial B_0}{\partial x} \right) \left(\int_{-H_0}^0 \hat{u}_{14} dz + \frac{1}{2} \hat{\gamma}_{14}^H \right) - \frac{1}{2B_0} \frac{\partial}{\partial x} \hat{\gamma}_{14}^B - \frac{1}{2} \hat{\zeta}_{14}^B. \quad (38b)$$

The associated boundary conditions are

$$\frac{\partial \hat{u}_{14}}{\partial z} = \frac{s_f}{\nu_T(x)} \hat{u}_{14} + \frac{1}{2} \hat{\chi}_{14}^H \quad \text{at } z = -H_0, \quad (39a)$$

$$\frac{\partial \hat{u}_{14}}{\partial z} = 0 \quad \text{at } z = 0 \quad (39b)$$

$$(39c)$$

with

$$\frac{1}{2} \hat{\gamma}_{14}^H = \frac{1}{2} \hat{H}_{12}(x, t) \hat{u}_{02}(x, t) \Big|_{z=-H_0} = 2 [\gamma^H] \quad (40)$$

$$\frac{1}{2} \hat{\gamma}_{14}^B = \frac{1}{2} \hat{B}_{12} \int_{-H_0}^0 \hat{u}_{02} dz = 2 [\gamma^B] \quad (41)$$

$$\frac{1}{2} \hat{\zeta}_{14}^B = \frac{1}{2} \frac{\hat{B}_{12}}{B_0} \frac{\partial \hat{\zeta}_{02}}{\partial t} = 2 [\zeta^B] \quad (42)$$

$$\frac{1}{2} \hat{\chi}_{14}^H = \frac{1}{2} \left(-\frac{s_f}{\nu_T} \hat{H}_{12} \frac{\partial \hat{u}_{02}}{\partial z} \Big|_{-H_0} + \hat{H}_{12} \frac{\partial^2 \hat{u}_{02}}{\partial z^2} \Big|_{-H_0} \right) = 2 [\chi^H] \quad (43)$$

The general solution to Eq. (38a), satisfying the boundary conditions is

$$\hat{u}_{14}(x, z) = \frac{g}{2i\sigma} (\alpha_{M4} \cosh(r_{M4}(x)z) - 1) \frac{\partial \hat{\zeta}_{14}}{\partial x} - \frac{1}{2} \frac{\nu_T}{s_f} \alpha_{M4} \hat{\chi}^H \cosh(r_{M4}(x)z) \quad (44)$$

with

$$r_{M4}(x) = \sqrt{\frac{2i\sigma}{\nu_T(x)}} \quad (45a)$$

$$\alpha_{M4} = \frac{s_f(x)}{r_{M4}(x) \nu_T(x) \sinh(r_{M4}(x)H_0) + s_f(x) \cosh(r_{M4}(x)H_0)}. \quad (45b)$$

Injecting Eq. (44) into Eq. (38b) gives the equation for the surface elevation, with four width or depth related forcing terms:

$$T_4 \frac{\partial^2 \hat{\zeta}_{14}}{\partial x^2} + \left(\frac{\partial T_4}{\partial x} + \frac{1}{B_0} \frac{\partial B_0}{\partial x} T_4 \right) \frac{\partial \hat{\zeta}_{14}}{\partial x} - \frac{4\sigma^2}{g} \hat{\zeta}_{14} = F_{\text{dips}} + F_{\text{depth}} + F_{\text{width}} + F_{\text{surf}} \quad (46)$$

with

$$T_4(x) = \frac{\alpha_{M_4}}{r_{M_4}} \sinh(r_{M_4}(x)H_0(x)) - H_0(x) \quad (47a)$$

$$F_{\text{dips}} = \frac{i\sigma}{g} \frac{\partial}{\partial x} \left(\frac{\nu_T \alpha_{M_4}}{s_f r_{M_4}} \hat{\chi}^H \sinh(r_{M_4}H_0) \right) + \frac{i\sigma}{g} \frac{1}{B_0} \frac{\partial B_0}{\partial x} \frac{\nu_T \alpha_{M_4}}{s_f r_{M_4}} \hat{\chi}^H \sinh(r_{M_4}H_0) \quad (47b)$$

$$F_{\text{depth}} = -\frac{i\sigma}{g} \left(\frac{\partial \hat{\gamma}^H}{\partial x} + \frac{1}{B_0} \frac{\partial B_0}{\partial x} \hat{\gamma}^H \right), \quad (47c)$$

$$F_{\text{width}} = -\frac{i\sigma}{g} \frac{1}{B_0} \frac{\partial \hat{\gamma}^B}{\partial x}, \quad (47d)$$

$$F_{\text{surf}} = -\frac{i\sigma}{g} \hat{\zeta}^B. \quad (47e)$$

3.4 Analytical solution for a horizontal bottom and an exponential width variation

3.4.1 Equations

To find fully analytical solutions for Eq. (46), we assume a constant eddy viscosity, a horizontal bottom, a constant bottom friction, and an exponentially decaying width

$$B_0(x) = B_s \exp\left(-\frac{x}{L_b}\right) \quad \text{such that} \quad \frac{1}{B_0} \frac{\partial B_0}{\partial x} = -\frac{1}{L_b}$$

with B_s the width at the sea boundary and L_b the estuarine convergence length. Additionally, the parameterization of B_0 and H_0 are

$$H_1 = -\frac{H_0}{b'} \zeta_{02} \quad (48a)$$

$$B_1 = \frac{B_0}{b'} \zeta_{02} \quad (48b)$$

where b' is a constant. Note that this parameterization is in agreement with Eqs (11) and (16) as long as

$$b' = 2A_{M_2} \frac{B_0}{\Delta B}. \quad (49)$$

These assumptions simplify Eq. (46) to

$$\frac{\partial^2 \hat{\zeta}_{14}}{\partial x^2} - \frac{1}{L_b} \frac{\partial \hat{\zeta}_{14}}{\partial x} - \frac{4\sigma^2}{gT_4} \hat{\zeta}_{14} = \frac{F_{\text{dips}}}{T_4} + \frac{F_{\text{depth}}}{T_4} + \frac{F_{\text{width}}}{T_4} + \frac{F_{\text{surf}}}{T_4}. \quad (50a)$$

$$F_{\text{dips}} = \frac{i\sigma \nu_T \alpha_{M_4}}{g s_f r_{M_4}} \sinh(r_{M_4}H_0) \left(\frac{\partial \hat{\chi}^H}{\partial x} - \frac{1}{L_b} \hat{\chi}^H \right) \quad (50b)$$

$$F_{\text{depth}} = -\frac{i\sigma}{g} \left(\frac{\partial \hat{\gamma}^H}{\partial x} - \frac{1}{L_b} \hat{\gamma}^H \right), \quad (50c)$$

$$F_{\text{width}} = -\frac{i\sigma}{gB_s} \exp\left(\frac{x}{L_b}\right) \frac{\partial \hat{\gamma}^B}{\partial x}, \quad (50d)$$

$$F_{\text{surf}} = -\frac{i\sigma}{g} \hat{\zeta}^B. \quad (50e)$$

3.4.2 Homogeneous solution

The general solution to Eqs 46 is

$$\hat{\zeta}_h(x) = K_1 \exp\left(\frac{x}{2L_b} - \frac{k_{M4}}{2}x\right) + K_2 \exp\left(\frac{x}{2L_b} + \frac{k_{M4}}{2}x\right) \quad (51)$$

where K_1 and K_2 are constants depending on the boundary conditions, and the complex wave number k_{M4} verifies

$$k_{M4} = \sqrt{\frac{1}{L_b^2} + \frac{16\sigma^2}{gT_4}} = \sqrt{\frac{1}{L_b^2} + \frac{16\sigma^2 r_{M4}}{g\alpha_{M4} \sinh(r_{M4}H_0) - gr_{M4}H_0}} \quad (52)$$

3.4.3 Particular solutions

To each forcing term corresponds a unique particular solution. It turns out that it is always possible to write the forcing of each particular solution under the same form, which we name the canonical form. The equations for the four different width or depth dependent forcing terms will be written in this canonical form in order to facilitate the determination of each particular solution. A possibility of such a canonical form is

$$\begin{aligned} \frac{\partial^2 \hat{\zeta}_p}{\partial x^2} - \frac{1}{L_b} \frac{\partial \hat{\zeta}_p}{\partial x} - \frac{4\sigma^2}{gT_4} \hat{\zeta}_p &= F_{\text{canon}}, \\ F_{\text{canon}} &= C_F \exp\left(\frac{x}{L_b}\right) \cosh(k_{M2}(x-L)) \\ &+ S_F \exp\left(\frac{x}{L_b}\right) \sinh(k_{M2}(x-L)) + E_F \exp\left(\frac{x}{L_b}\right), \end{aligned} \quad (53)$$

where the canonical forcing term F_{canon} refers either to F_{dips} , F_{depth} , F_{width} or F_{surf} , and the constants C_F , S_F and E_F can be filled in accordingly. The particular solution then takes the form

$$\hat{\zeta}_{\text{part}} = C_S \exp\left(\frac{x}{L_b}\right) \cosh(k_{M2}(x-L)) + S_S \exp\left(\frac{x}{L_b}\right) \sinh(k_{M2}(x-L)) + E_S \exp\left(\frac{x}{L_b}\right), \quad (54)$$

where the constants C_S , S_S and E_S read

$$S_S = \frac{\frac{k_{M2}}{L_b} C_F - \left(k_{M2}^2 - \frac{4\sigma^2}{gT_4}\right) S_F}{\frac{k_{M2}^2}{L_b^2} - \left(k_{M2}^2 - \frac{4\sigma^2}{gT_4}\right)^2}, \quad (55)$$

$$C_S = \frac{\frac{k_{M2}}{L_b} S_F - \left(k_{M2}^2 - \frac{4\sigma^2}{gT_4}\right) C_F}{\frac{k_{M2}^2}{L_b^2} - \left(k_{M2}^2 - \frac{4\sigma^2}{gT_4}\right)^2}, \quad (56)$$

$$E_S = -\frac{gT_4}{4\sigma^2} E_F. \quad (57)$$

For details about the calculation method of the constants, the reader is referred to Appendix A1.1

3.4.4 Total solution

The total solution obviously consists of the sum of the homogeneous solution and the particular solution,

$$\hat{\zeta}_{14}(x) = \hat{\zeta}_h(x) + \hat{\zeta}_p(x). \quad (58)$$

The integration constant K_1 and K_2 can now be determined using the boundary conditions $\hat{\zeta}_{14} = 0$ and $\partial\hat{\zeta}_{14}/\partial x(L) = 0$. The computation of K_1 and K_2 is detailed in Appendix, and leads to

$$K_1 = \frac{\lambda_3 - \lambda_2\lambda_4}{\lambda_1 - \lambda_2}, \quad (59a)$$

$$K_2 = \frac{\lambda_3 - \lambda_1\lambda_4}{\lambda_2 - \lambda_1}. \quad (59b)$$

The parameters λ_1 , λ_2 , λ_3 and λ_4 were introduced for conciseness and read

$$\lambda_1 = \left(\frac{1}{2L_b} - \frac{k_{M4}}{2} \right) \exp\left(\frac{L}{2L_b} - \frac{k_{M4}L}{2} \right), \quad (60a)$$

$$\lambda_2 = \left(\frac{1}{2L_b} + \frac{k_{M4}}{2} \right) \exp\left(\frac{L}{2L_b} + \frac{k_{M4}L}{2} \right), \quad (60b)$$

$$\lambda_3 = -\exp\left(\frac{L}{L_b} \right) \left(\frac{C_S + E_S}{L_b} + S_S k_{M2} \right), \quad (60c)$$

$$\lambda_4 = -S_S \sinh(-k_{M2}L) - C_S \cosh(-k_{M2}L) - E_S. \quad (60d)$$

3.4.5 Individual forcing terms

In the case of a horizontal bottom and an exponentially converging width, it is possible to have a fully analytical expression of the forcing terms. Since the forcing terms (between brackets, $[\cdot]$) depend on the leading order variables u_0 and/or ζ_{02} , an analytical expression of these quantities is required. Under the assumptions stated in the beginning of this section, the equations governing the leading order variables, Eqs (7a-7b), admit fully analytical solutions. According to Wei *et al.*, 2016, the analytical solution for u_0 , ζ_{02} and $\partial\zeta_{02}/\partial x$ under the present assumptions are

$$\hat{u}_0 = \frac{g}{i\sigma} (\alpha_{M2} \cosh(r_{M2}z) - 1) \frac{\partial\zeta_{02}}{\partial x}, \quad (61a)$$

$$\hat{\zeta}_0 = C_{M2} \exp\left(\frac{x}{2L_b} \right) \left(-\sinh\left(\frac{k_{M2}}{2}(x-L) \right) + L_b k_{M2} \cosh\left(\frac{k_{M2}}{2}(x-L) \right) \right), \quad (61b)$$

with,

$$r_{M2} = \sqrt{\frac{i\sigma}{\nu_T}}, \quad (62a)$$

$$\alpha_{M2} = \frac{s_f}{\nu_T r_{M2} \sinh(r_{M2}H_0) + s_f \cosh(r_{M2}H_0)}, \quad (62b)$$

$$k_{M2} = \sqrt{\frac{1}{L_b^2} + \frac{4\sigma^2 r_{M2}}{g(\alpha_{M2} \sinh(r_{M2}H_0) - r_{M2}H_0)}}, \quad (62c)$$

$$C_{M2} = \frac{A_{M2}}{\sinh\left(\frac{k_{M2}L}{2} \right) + k_{M2}L_b \cosh\left(\frac{k_{M2}L}{2} \right)}. \quad (62d)$$

F_{dips}

The starting point for the development of F_{dips} is

$$\frac{F_{\text{dips}}}{T_4} = \frac{i\sigma}{gT_4} \frac{\nu_T}{s_f} \frac{\alpha_{M4}}{r_{M4}} \sinh(r_{M4}H_0) \left(\frac{\partial\hat{\chi}^H}{\partial x} - \frac{1}{L_b} \hat{\chi}^H \right) \quad (63)$$

Using the definition of $\hat{\chi}^H$, Eq. (43), this equation can be rewritten

$$\frac{F_{\text{dips}}}{T_4} = \frac{i\sigma}{gT_4} \frac{\nu_T}{s_f} \frac{\alpha_{M_4}}{r_{M_4}} \sinh(r_{M_4} H_0) \left(\frac{\partial}{\partial x} \left(-\frac{s_f}{\nu_T} \hat{H}_1 \frac{\partial \hat{u}_0}{\partial z} \Big|_{-H_0} + \hat{H}_1 \frac{\partial^2 \hat{u}_0}{\partial z^2} \Big|_{-H_0} \right) - \frac{1}{L_b} \left(-\frac{s_f}{\nu_T} \hat{H}_1 \frac{\partial \hat{u}_0}{\partial z} \Big|_{-H_0} + \hat{H}_1 \frac{\partial^2 \hat{u}_0}{\partial z^2} \Big|_{-H_0} \right) \right) \quad (64)$$

or

$$\frac{F_{\text{dips}}}{T_4} = \frac{i\sigma}{gT_4} \frac{\nu_T}{s_f} \frac{\alpha_{M_4}}{r_{M_4}} \sinh(r_{M_4} H_0) \left(\frac{\partial}{\partial x} - \frac{1}{L_b} \right) \left(-\frac{s_f}{\nu_T} \hat{H}_1 \frac{\partial \hat{u}_0}{\partial z} \Big|_{-H_0} + \hat{H}_1 \frac{\partial^2 \hat{u}_0}{\partial z^2} \Big|_{-H_0} \right) \quad (65)$$

Finally,

$$\frac{F_{\text{dips}}}{T_4} = -C_{M_2}^2 \frac{\nu_T}{s_f} \frac{r_{M_2}}{r_{M_4}} \frac{\alpha_{M_2} \alpha_{M_4}}{T_4} \frac{H_0}{b'} \sinh(r_{M_4} H_0) \left(\frac{s_f}{\nu_T} \sinh(r_{M_2} H_0) + r_{M_2} \cosh(r_{M_2} H_0) \right) \exp\left(\frac{x}{L_b}\right) \left(\left(-\frac{k_{M_2}^2}{4} + \frac{k_{M_2}^4 L_b^2}{4} \right) \cosh(k_{M_2}(x-L)) + \left(-\frac{L_b k_{M_2}^3}{4} + \frac{k_{M_2}}{4L_b} \right) \sinh(k_{M_2}(x-L)) \right) \quad (66)$$

The final expression for F_{depth} can be found using the expressions of the derivatives of ζ_{02} , given in Appendix A1.3,

F_{depth}

The starting point for the development of F_{depth} is

$$\frac{F_{\text{depth}}}{T_4} = -\frac{i\sigma}{gT_4} \left(\frac{\partial \hat{\gamma}^H}{\partial x} - \frac{1}{L_b} \hat{\gamma}^H \right). \quad (67)$$

Using the definition of $\hat{\gamma}^H$, Eq. (40), this equation can be rewritten

$$\frac{F_{\text{depth}}}{T_4} = -\frac{i\sigma}{gT_4} \left(\frac{\partial}{\partial x} \left(\hat{H}_1 \hat{u}_0 \Big|_{z=-H_0} \right) - \frac{1}{L_b} \hat{H}_1 \hat{u}_0 \Big|_{z=-H_0} \right).$$

Injecting the expression for H_1 , i.e. Eq. (48a), the formulation becomes

$$\frac{F_{\text{depth}}}{T_4} = -\frac{i\sigma}{gT_4} \left(-\frac{\partial}{\partial x} \left(\frac{H_0}{b'} \hat{\zeta}_0 \hat{u}_0 \Big|_{z=-H_0} \right) + \frac{1}{L_b} \frac{H_0}{b'} \hat{\zeta}_0 \hat{u}_0 \Big|_{z=-H_0} \right).$$

The combination with the formula for the leading order velocity u_0 , i.e. Eq. (61a), yields

$$\frac{F_{\text{depth}}}{T_4} = \frac{i\sigma}{gT_4} \frac{H_0}{b'} \left(\frac{\partial}{\partial x} \left(\frac{g}{i\sigma} (\alpha_{M_2} \cosh(-r_{M_2} H_0) - 1) \hat{\zeta}_0 \frac{\partial \hat{\zeta}_0}{\partial x} \right) - \frac{1}{L_b} \frac{g}{i\sigma} (\alpha_{M_2} \cosh(-r_{M_2} H_0) - 1) \hat{\zeta}_0 \frac{\partial \hat{\zeta}_0}{\partial x} \right)$$

$$\frac{F_{\text{depth}}}{T_4} = \frac{H_0}{b'T_4} (\alpha_{M_2} \cosh(-r_{M_2} H_0) - 1) \left(\left(\frac{\partial \hat{\zeta}_0}{\partial x} \right)^2 + \hat{\zeta}_0 \frac{\partial^2 \hat{\zeta}_0}{\partial x^2} - \frac{1}{L_b} \hat{\zeta}_0 \frac{\partial \hat{\zeta}_0}{\partial x} \right).$$

The final expression for F_{depth} can be found using the expressions of the derivatives of ζ_{02} , given in Appendix A1.3,

$$\frac{F_{\text{depth}}}{T_4} = C_{M_2}^2 \frac{H_0}{b'T_4} (\alpha_{M_2} \cosh(-r_{M_2} H_0) - 1) \exp\left(\frac{x}{L_b}\right) \left(\left(\frac{L_b^2 k_{M_2}^4}{4} - \frac{k_{M_2}^2}{4} \right) \cosh(k_{M_2}(x-L)) + \left(-\frac{L_b k_{M_2}^3}{4} + \frac{k_{M_2}}{4L_b} \right) \sinh(k_{M_2}(x-L)) \right) \quad (68)$$

F_{width}

The starting point for the development of F_{width} is

$$\frac{F_{\text{width}}}{T_4} = -\frac{i\sigma}{gB_s T_4} \exp\left(\frac{x}{L_b}\right) \frac{\partial \hat{\gamma}^B}{\partial x} \quad (69)$$

Using the definition of $\hat{\gamma}^B$, Eq. (41), this equation can be rewritten

$$\frac{F_{\text{width}}}{T_4} = -\frac{i\sigma}{gB_s T_4} \exp\left(\frac{x}{L_b}\right) \frac{\partial}{\partial x} \left(\hat{B}_1 \int_{-H_0}^0 \hat{u}_0 dz \right) \quad (70)$$

Injecting the expression for B_1 , i.e. Eq. (48b), the formulation becomes

$$\frac{F_{\text{width}}}{T_4} = -\frac{i\sigma}{gb' T_4} \left(-\frac{\hat{\zeta}_0}{L_b} + \frac{\partial \hat{\zeta}_0}{\partial x} + \hat{\zeta}_0 \frac{\partial}{\partial x} \right) \int_{-H_0}^0 \hat{u}_0 dz. \quad (71)$$

After some math, we obtain

$$\frac{F_{\text{width}}}{T_4} = -\frac{i\sigma}{gb' T_4} \frac{T_2}{T_4} \left(\left(\frac{\partial \hat{\zeta}_0}{\partial x} \right)^2 + \hat{\zeta}_0 \frac{\partial^2 \hat{\zeta}_0}{\partial x^2} - \frac{1}{L_b} \hat{\zeta}_0 \frac{\partial \hat{\zeta}_0}{\partial x} \right), \quad (72)$$

with

$$T_2(x) = \frac{\alpha_{M2}}{r_{M2}} \sinh(r_{M2}(x)H_0(x)) - H_0(x). \quad (73)$$

The final expression for F_{depth} can be found using the expressions of the derivatives of ζ_{02} , given in Appendix A1.3,

$$\frac{F_{\text{width}}}{T_4} = -\frac{C_{M2}^2 T_2}{b' T_4} \exp\left(\frac{x}{L_b}\right) \left(\left(-\frac{k_{M2}^2}{4} + \frac{k_{M2}^4 L_b^2}{4} \right) \cosh(k_{M2}(x-L)) + \left(-\frac{L_b k_{M2}^3}{4} + \frac{k_{M2}}{4L_b} \right) \sinh(k_{M2}(x-L)) \right) \quad (74)$$

 F_{surf}

The starting point for the development of F_{surf} is

$$\frac{F_{\text{surf}}}{T_4} = -\frac{i\sigma}{gT_4} \hat{\zeta}^B. \quad (75)$$

Using the definition of $\hat{\zeta}^B$, Eq. (42), this equation can be rewritten

$$\frac{F_{\text{surf}}}{T_4} = -\frac{i\sigma}{gT_4} \frac{\hat{B}_1}{B_0} \frac{\partial \hat{\zeta}_0}{\partial t}. \quad (76)$$

Expliciting the complex time-derivative of $\hat{\zeta}^B$ and the parameterization of the width variation, Eq. (48b),

$$\frac{F_{\text{surf}}}{T_4} = \frac{\sigma^2}{gT_4 b'} \hat{\zeta}_0^2 \quad (77)$$

Finally, using Eq. (87e),

$$\frac{F_{\text{surf}}}{T_4} = \frac{C_{M2}^2}{2} \frac{\sigma^2}{gT_4 b'} \hat{\zeta}_0^2 \exp\left(\frac{x}{L_b}\right) \left((L_b k_{M2})^2 - 1 + (1 + k_{M2}^2 L_b^2) \cosh(k_{M2}(x-L)) - 2L_b k_{M2} \sinh(k_{M2}(x-L)) \right) \quad (78)$$

4 Simulation results

The new, width or depth dependent, forcing terms have been implemented in iFlows semi-analytical and numerical modules. In this report, we only focus on the resulting additional water elevation at M4 frequency. These elevations are more difficult to implement as compared to the M0 water elevations, and are believed to be important contributors to the M4 tidal signal in the Scheldt. The depth and width dependent water elevations at M0 frequency, the additional residual velocities and the additional M4 tidal velocities are analyzed in a follow up project. In the semi-analytical solver, the second order equation for the surface-elevation (i.e. Eq. (46)) is integrated numerically while the solution for the velocity is still given by Eq. (44). In the numerical solver both the velocity and the surface elevation are computed numerically. Additionally to these two solvers, a fully analytical solver was created for estuary models with a horizontal bottom and an exponentially converging width.

4.1 Validation

We choose to take advantage of these three solvers, to verify the implementations of the forcing terms related to width and depth variations, Eqs (47b-47e). The configuration used for the validation was one with a horizontal bottom and an exponential converging width. The parameter values are largely inspired by the parameter values for the Scheldt by Wei *et al.*, 2016 and given in Table 1. The aim is to validate the implement-

Table 1 – Parameter values for an idealized Scheldt model (Wei *et al.*, 2016).

| A_{M_2} (m) | A_{M_4} (m) | L (km) | B_s (m) | b (km) | H_0 (m) | Q_1 (m ³ s ⁻¹) | ν_T (m ² s ⁻¹) | s_f (m s ⁻¹) |
|---------------|---------------|----------|-----------|----------|-----------|---|---|----------------------------|
| 2.00 | 0.20 | 200 | 4000 | 50 | 10 | 90 | 0.0099 | 0.0085 |

ation of the width and depth dependent terms contributing to the first order surface elevation. Accordingly, the leading order surface elevation and velocity are computed with the same semi-analytical solver, regardless if the first order solver is numerical, semi-analytical or fully analytical. In this way, any possible discrepancies between the solutions at leading order is not influencing the solutions at first order.

The relative performances of the semi-analytical, analytical and numerical solvers are showed in Figs 2, 3 and 4. Quadratic convergence was checked by refining the grid 10 times in the horizontal and vertical directions. The error between two solvers, defined as

$$\left| \frac{\zeta_{solver1} - \zeta_{solver2}}{\zeta_{solver1}} \right|, \quad (79)$$

is reduced by two orders of magnitude for ζ_{depth} , ζ_{width} and ζ_{surf} , when the grid is refined by one order of magnitude. The relative error between the ζ_{dips} values computed by different solvers only reduces by one order of magnitude for a reason yet unknown.

The relative behavior of the solvers is similar when the phase is analyzed. As illustration, the phases computed with the fully analytical method and the numerical method are displayed in Fig. 5. The phases of ζ_{depth} , ζ_{width} and ζ_{surf} converge quadratically while the phase of ζ_{dips} converges linearly. These results give confidence in the correct implementation of the forcing terms in iFlow, even if the non-quadratic convergence for ζ_{dips} needs to be clarified.

Figure 2 – Evolution of the differences in water levels computed by the semi-analytical and the fully analytical solver (configuration of Wei *et al.*, 2016).

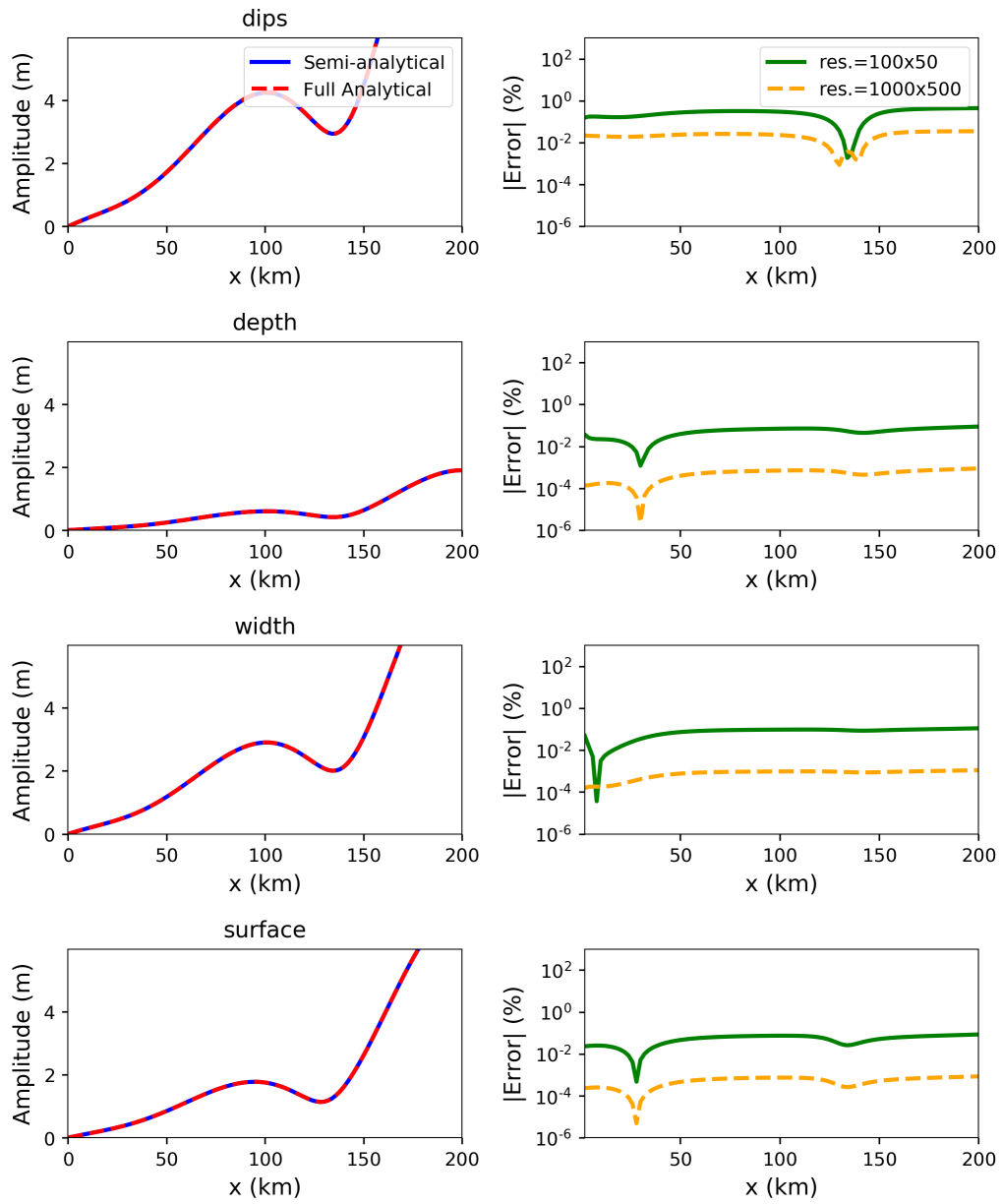


Figure 3 – Evolution of the differences in water levels computed by the numerical and the fully analytical solver (configuration of Wei *et al.*, 2016).

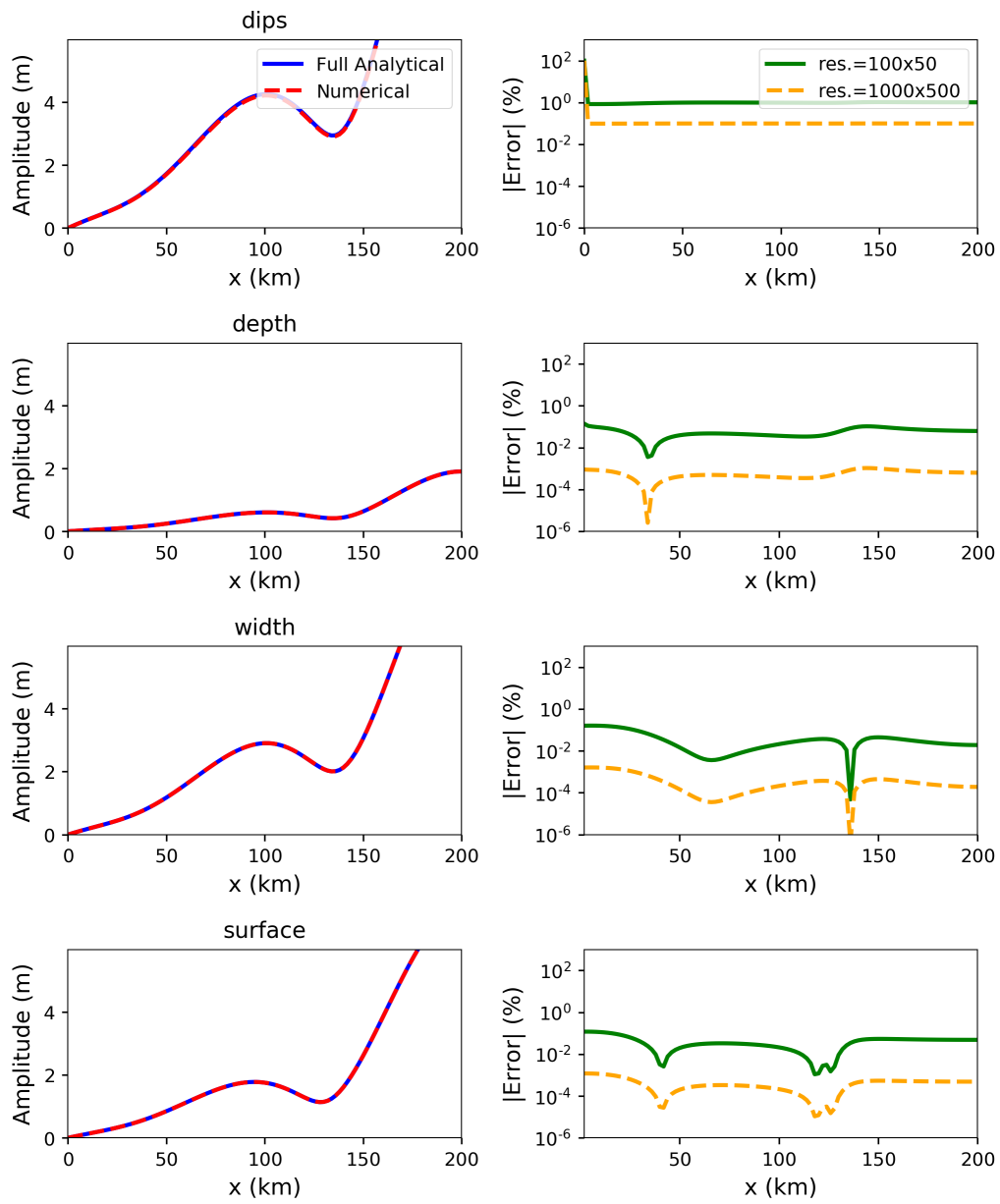


Figure 4 – Evolution of the differences in water levels computed by the numerical and the semi-analytical solver (configuration of Wei *et al.*, 2016).

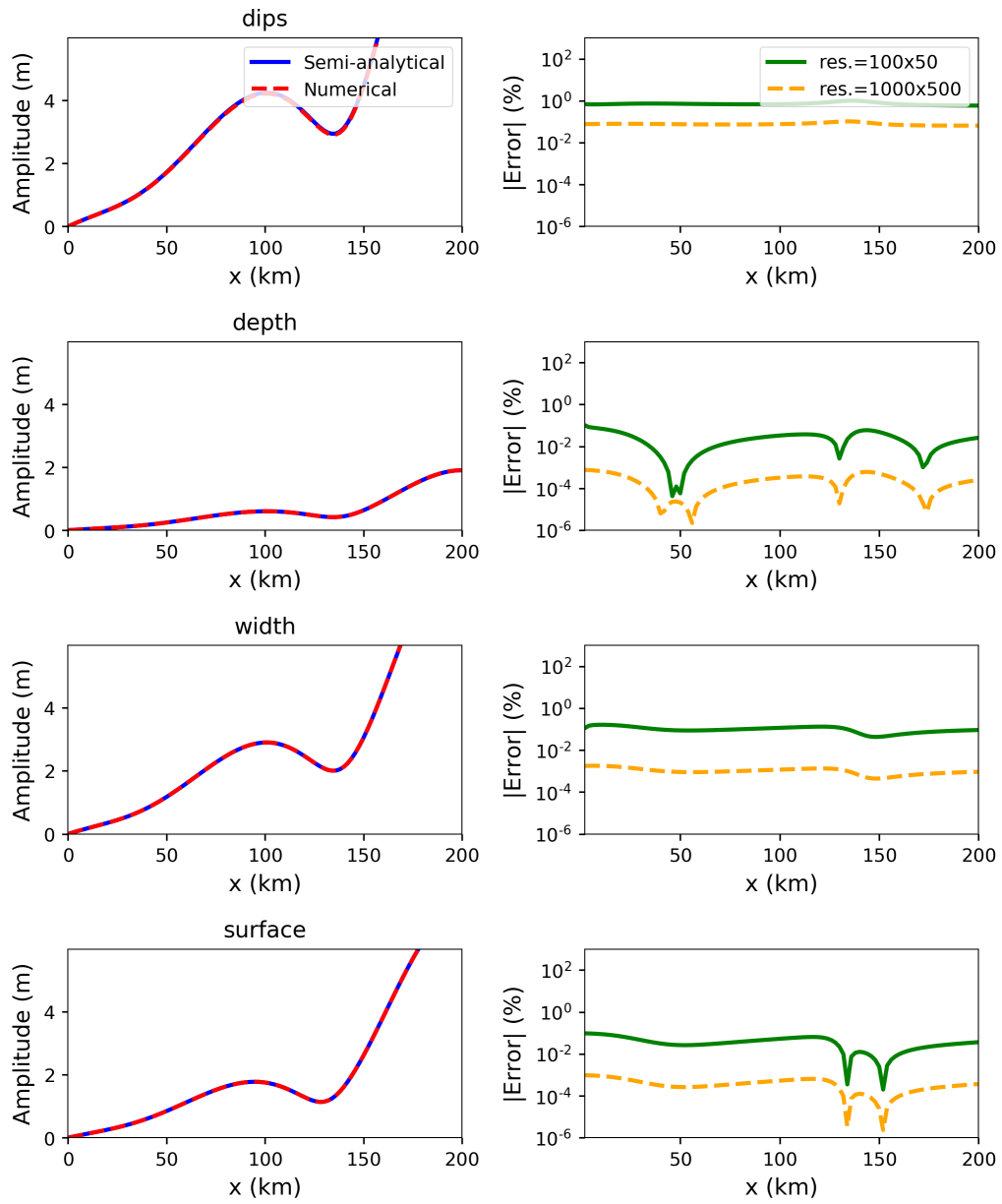
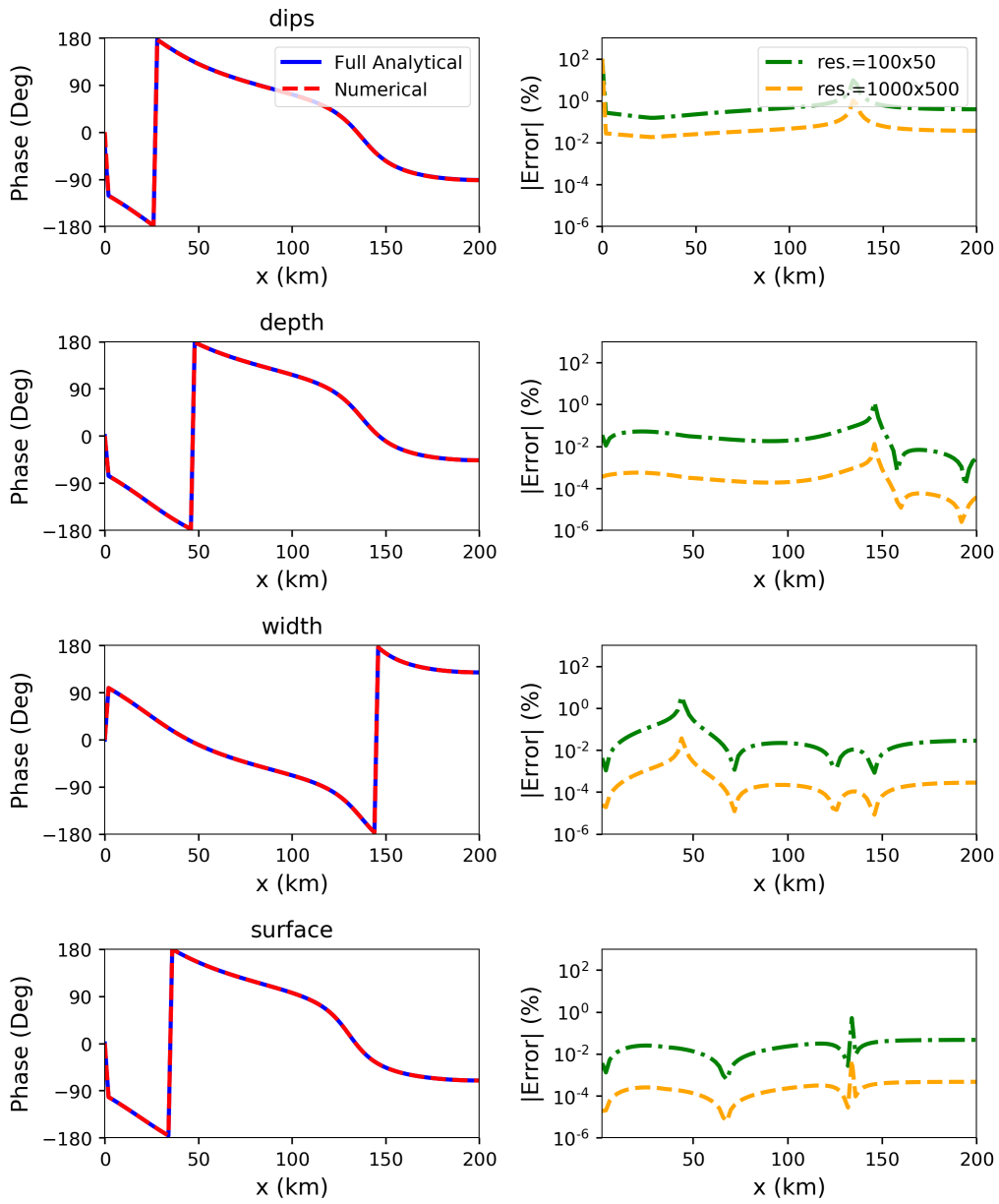


Figure 5 – Evolution of the differences in water levels computed by the numerical and the fully analytical solver (configuration of Wei *et al.*, 2016).



4.2 Effect of the incorporation of intertidal zones on the total M4 surface elevation (horizontal bottom)

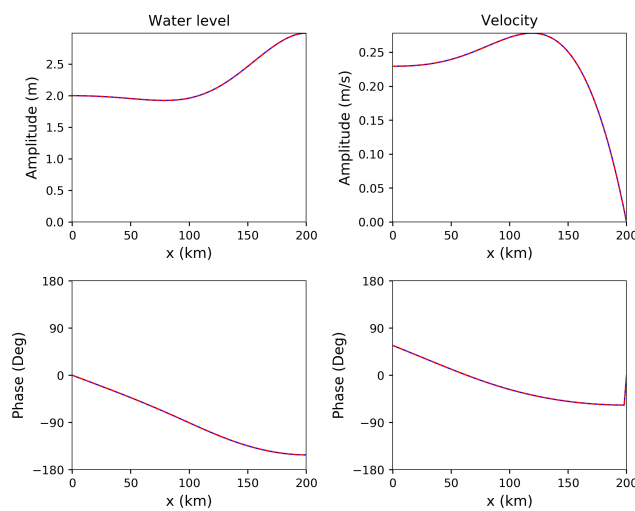
In the previous section, it is shown that the implementation of the forcing due to intertidal width and depth variations leads to converging results for all the width and depth dependent terms. As a result, we can now analyze with confidence the relative effect of depth and width dependent surface elevations with respect to the total M4 surface elevation. However, the first order forcing terms depend on the velocity and surface elevation at leading order. Additionally, particularly the bathymetry of the Scheldt is highly idealized in the current model and this property can significantly influence the leading order results. As a result, we will first study the surface elevation and bottom velocity at leading order, in the Wei *et al.*, 2016 configuration and in the Brouwer *et al.*, 2017 configuration (more details in Table 2).

Table 2 – Parameter values for a different idealized Scheldt model Brouwer *et al.*, 2017. Note that these parameters also include a phase shift of -1.3° between the external M4 and the external M2 tides.

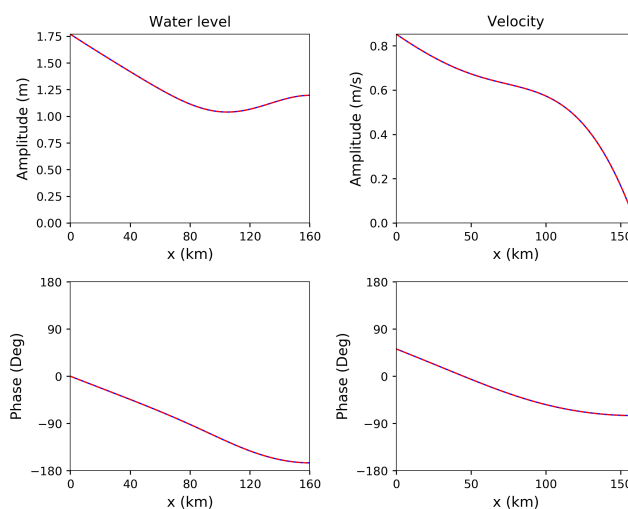
| A_{M_2} (m) | A_{M_4} (m) | L (km) | B_s (m) | b (km) | H_0 (m) | Q_1 ($\text{m}^3 \text{s}^{-1}$) | ν_T ($\text{m}^2 \text{s}^{-1}$) | s_f (m s^{-1}) |
|---------------|---------------|----------|-----------|----------|-----------|--------------------------------------|--|-----------------------------|
| 1.77 | 0.14 | 160 | 6000 | 50 | 10 | 90 | 0.061 | 0.003 |

The leading order surface elevation and the leading order bottom velocity are displayed in Figs 6 and 7. The expected evolution of the M2 surface elevation, i.e. a steady increase of the M2 amplitude until km 120 followed by a drop of the amplitude towards the weir (see measurement data in Brouwer *et al.*, 2017), is not reproduced by neither of the two models. Particularly, towards the end of the estuary, the amplitude of the M2 is about 3m with respect to a depth of 10m for the Wei *et al.*, 2016 parameter settings. The M2 surface elevation obtained using the Brouwer *et al.*, 2017 parameter settings is better at the upstream side of the estuary, with an elevation of about 1.75m. However, it also lacks the maximum around km 120. The amplitude of the bottom velocity predicted by Brouwer *et al.*, 2017 are much smaller than the one produced by Wei *et al.*, 2016, which is explained by the large friction coefficient of the latter with respect to the former. Both the phase of the surface elevation and the phase of the velocity seem to be of inverse sign with respect to the measured data.

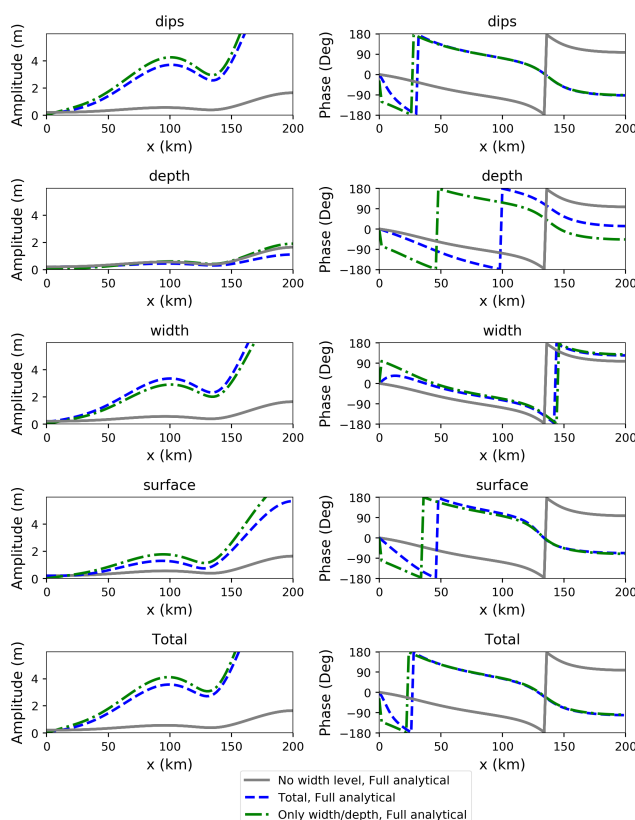
Figure 6 – Leading order solutions for the water level and the bottom velocity for the Wei *et al.*, 2016 configuration.



The leading order results show already quite some discrepancies with respect to the measurements. This feature implies that the first order results will probably show the same, if not a larger, difference with the measurements. However, we can still estimate the relative impact intertidal zones could have on the tidal signal. In this regard, it is for example particularly interesting to investigate the F_{dips} and the F_{depth} term, since

Figure 7 – Leading order solutions for the water level and the bottom velocity for the Brouwer *et al.*, 2017 configuration.


they are strongly dependent on the bottom velocity.

 Figure 8 – First order surface elevation decomposed into separate width-depth contributions (Wei *et al.*, 2016) (only full analytical results).


The different width and depth dependent M4 surface elevation components are displayed in Fig. 8 for the Wei *et al.*, 2016 configuration, in Fig. 9 for the Brouwer *et al.*, 2017 configuration. Every figure also contains the total M4 signal, with and without intertidal terms. As expected, the ζ_{depth} term is much smaller in the Wei *et al.*, 2016 configuration than in the Brouwer *et al.*, 2017 configuration due to larger friction. However, for the ζ_{dips} term, the opposite is true, probably due to higher gradients close to the wall in case of higher friction. Figure 9 and Fig. 8 also prove the phase is crucial for the damping or amplifying effects of the M4 components

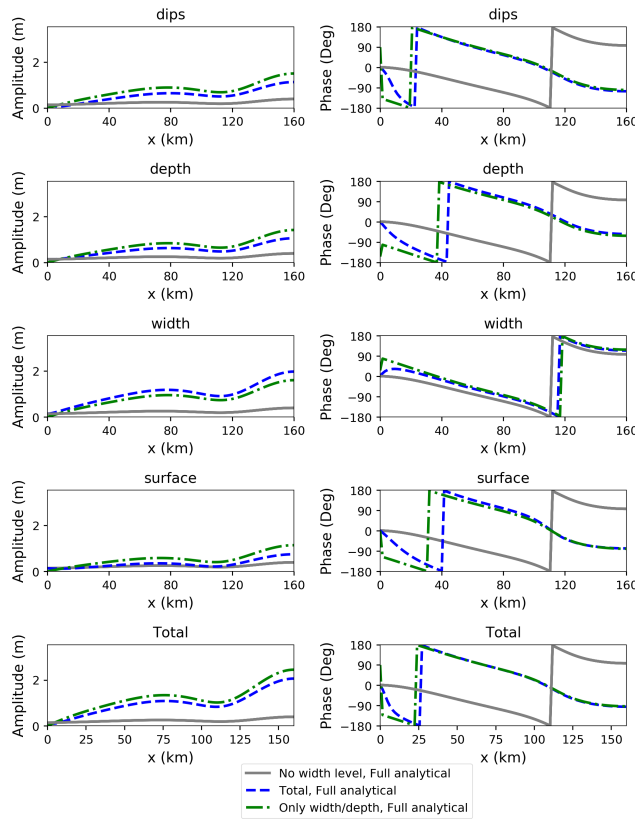
Figure 9 – First order surface elevation decomposed into separate width-depth contributions (Wei *et al.*, 2016) (only full analytical results).


Table 3 – Coefficients for the polynomial approximation of the water depth.

| d_1 | d_2 | d_3 |
|---|--|---|
| $-2.9013 \times 10^{-24} \text{m}^{-4}$ | $1.4030 \times 10^{-18} \text{m}^{-3}$ | $-2.4218 \times 10^{-13} \text{m}^{-2}$ |
| d_4 | d_5 | d_6 |
| $1.7490 \times 10^{-8} \text{m}^{-1}$ | -5.21410×10^{-4} | 15.332m |

generated by intertidal effects. Indeed, opposite phases but similar amplitudes cause the ζ_{depth} term to damp the overall M4 tide in the Wei *et al.*, 2016 case (see Fig. 8).

4.3 Case of a varying bottom

The case of a varying bottom has also been investigated. The depth H_0 is now a polynomial function of the fifth order

$$H_0(x) = d_1 x^5 + d_2 x^4 + d_3 x^3 + d_4 x^2 + d_5 x + d_6 \quad (80)$$

where the coefficient b_i are taken from Brouwer *et al.*, 2017 and given in Table 3

The comparison of the solutions obtained at first order by the semi-analytical solver and the numerical solver shows that the ζ_{depth} now converges linearly instead of quadratically and that the ζ_{dips} term does not converge with increasing grid resolution. However, the relative difference between the numerical solution and the semi-analytical solution is of order 1% or lower. Nevertheless, quadratic convergence is expected and these discrepancies need to be elucidated

4.4 Conclusion

Four width and dependent forcings of the M4 tide were implemented in iFlow's numerical and semi-analytical modules. An additional full analytical module was created for horizontal bottom and exponential width configurations. For the horizontal bottom configurations, the error between the solutions computed by different solvers converges for increasing grid resolution proving accurate implementation. In the non-horizontal bottom configuration, one of the terms does not converge. However, the error is small (order 1%). A first analysis of the solutions shows that width and depth variations, or intertidal zones, are significant contributors to the M4 surface elevations. The model is now operational for an investigation with a more realistic bathymetry as well as a more realistic first order width and depth parameterisation. This investigation should take place in a follow-up project and should clarify if the discrepancies between measured M4 amplitudes and modeled M4 amplitudes (in iFlow) can be eliminated by the incorporation of intertidal zones in iFlow.

References

- Brouwer, R. L.; Schramkowski, G. P.; Dijkstra, Y. M.; Schuttelaars, H. M.** (2018). Time Evolution of Estuarine Turbidity Maxima in Well-Mixed, Tidally Dominated Estuaries: The Role of Availability- and Erosion-Limited Conditions. *Journal of Physical Oceanography* 48 (8): 1629–1650
- Brouwer, T.; Schramkowski, G.; Mostaert, F.** (2017). Geïdealiseerde processtudie van systeemovergangen naar hypertroebelheid. 2.0. *WL Rapporten*, 13_103_3. Flanders Hydraulics Research: Antwerp, Belgium
- Chernetsky, A. S.; Schuttelaars, H. M.; Talke, S. A.** (2010). The effect of tidal asymmetry and temporal settling lag on sediment trapping in tidal estuaries. *Ocean Dynamics* 60 (5): 1219–1241
- Dijkstra, Y. M.; Brouwer, R. L.; Schuttelaars, H. M.; Schramkowski, G. P.** (2017). The iFlow modelling framework v2. 4: a modular idealized process-based model for flow and transport in estuaries. *Geoscientific Model Development* 10 (7): 2691–2713
- Dijkstra, Y. M.; Schuttelaars, H. M.; Schramkowski, G. P.** (2019a). A Regime Shift From Low to High Sediment Concentrations in a Tide-Dominated Estuary. *Geophysical Research Letters* 46 (8): 4338–4345
- Dijkstra, Y. M.; Schuttelaars, H. M.; Schramkowski, G. P.; Brouwer, R. L.** (2019b). Modeling the Transition to High Sediment Concentrations as a Response to Channel Deepening in the Ems River Estuary. *124* (3): 1578–1594
- Wei, X.; Schramkowski, G. P.; Schuttelaars, H. M.** (2016). Salt dynamics in well-mixed estuaries: Importance of advection by tides. *Journal of Physical Oceanography* 46 (5): 1457–1475

A1 Intermediate steps for the computation of the width/depth dependent M4

A1.1 Resolution method for the particular solution

The total solution of Eq. (50a) consists of the sum of a homogeneous solution, given by Eq. (51), and a particular solution for each forcing term. The particular solutions are assumed to be of the form given by Eq. (54). As a reminder, this solution is written

$$\zeta_{\text{part}} = C_S \exp\left(\frac{x}{L_b}\right) \cosh(k_{M2}(x-L)) + S_S \exp\left(\frac{x}{L_b}\right) \sinh(k_{M2}(x-L)) + E_S \exp\left(\frac{x}{L_b}\right),$$

Accordingly, the derivatives of the assumed analytical solution are

$$\begin{aligned} \frac{\partial \zeta}{\partial x} &= \left(\frac{S_S}{L_b} + k_{M2} C_S\right) \exp\left(\frac{x}{L_b}\right) \sinh(k_{M2}(x-L)) \\ &+ \left(\frac{C_S}{L_b} + k_{M2} S_S\right) \exp\left(\frac{x}{L_b}\right) \cosh(k_{M2}(x-L)) + \frac{E_S}{L_b} \exp\left(\frac{x}{L_b}\right), \end{aligned} \quad (81a)$$

$$\begin{aligned} \frac{\partial^2 \zeta}{\partial x^2} &= \left(\left(\frac{1}{L_b^2} + k_{M2}^2\right) S_S + 2\frac{k_{M2}}{L_b} C_S\right) \exp\left(\frac{x}{L_b}\right) \sinh(k_{M2}(x-L)) \\ &+ \left(\left(\frac{1}{L_b^2} + k_{M2}^2\right) C_S + 2\frac{k_{M2}}{L_b} S_S\right) \exp\left(\frac{x}{L_b}\right) \cosh(k_{M2}(x-L)) + \frac{E_S}{L_b^2} \exp\left(\frac{x}{L_b}\right). \end{aligned} \quad (81b)$$

By injecting Eqs (54), (81a) and (81b) into Eq. (53), finding the constant C_S , S_S and E_S is equivalent to resolving

$$\left(\left(k_{M2}^2 - \frac{4\sigma^2}{gT_4}\right) S_S + \frac{k_{M2}}{L_b} C_S\right) = S_F, \quad (82a)$$

$$\left(\left(k_{M2}^2 - \frac{4\sigma^2}{gT_4}\right) C_S + \frac{k_{M2}}{L_b} S_S\right) = C_F, \quad (82b)$$

$$-\frac{4\sigma^2}{gT_4} E_S = E_F. \quad (82c)$$

such that finally

$$S_S = \frac{\frac{k_{M2}}{L_b} C_F - \left(k_{M2}^2 - \frac{4\sigma^2}{gT_4}\right) S_F}{\frac{k_{M2}^2}{L_b^2} - \left(k_{M2}^2 - \frac{4\sigma^2}{gT_4}\right)^2}$$

$$C_S = \frac{\frac{k_{M2}}{L_b} S_F - \left(k_{M2}^2 - \frac{4\sigma^2}{gT_4}\right) C_F}{\frac{k_{M2}^2}{L_b^2} - \left(k_{M2}^2 - \frac{4\sigma^2}{gT_4}\right)^2}$$

$$E_S = -\frac{gT_4}{4\sigma^2} E_F$$

A1.2 Integration constants of the homogeneous solution

The total analytical solution, i.e. the sum of the homogeneous and the particular solution, is

$$\begin{aligned} \hat{\zeta}_{14} = & K_1 \exp\left(\frac{x}{2L_b} - \frac{k_{M4}}{2}x\right) + K_2 \exp\left(\frac{x}{2L_b} + \frac{k_{M4}}{2}x\right) \\ & + C_S \exp\left(\frac{x}{L_b}\right) \cosh(k_{M2}(x-L)) + S_S \exp\left(\frac{x}{L_b}\right) \sinh(k_{M2}(x-L)) + E_S \exp\left(\frac{x}{L_b}\right). \end{aligned} \quad (83)$$

In this solution, the constants K_1 and K_2 can be computed, using the boundary conditions. The imposed surface elevation at $x = 0$, i.e. $\hat{\zeta}_{14}(0) = 0$ gives

$$K_1 + K_2 + C_S \cosh(-k_{M2}L) + S_S \cosh(-k_{M2}L) + E_S = 0. \quad (84)$$

The imposed flow-rate at $x = L$ translates into $\partial\hat{\zeta}_{14}/\partial z = 0$.

$$\begin{aligned} K_1 \left(\frac{1}{2L_b} - \frac{k_{M4}}{2}\right) \exp\left(\frac{L}{2L_b} - \frac{k_{M4}}{2}L\right) + K_2 \left(\frac{1}{2L_b} + \frac{k_{M4}}{2}\right) \exp\left(\frac{L}{2L_b} + \frac{k_{M4}}{2}L\right) \\ + \left(\frac{C_S}{L_b} + S_S k_{M2} + \frac{E_S}{L_b}\right) \exp\left(\frac{L}{L_b}\right) = 0 \end{aligned} \quad (85)$$

By posing

$$\begin{aligned} \lambda_1 &= \left(\frac{1}{2L_b} - \frac{k_{M4}}{2}\right) \exp\left(\frac{L}{2L_b} - \frac{k_{M4}}{2}L\right), \\ \lambda_2 &= \left(\frac{1}{2L_b} + \frac{k_{M4}}{2}\right) \exp\left(\frac{L}{2L_b} + \frac{k_{M4}}{2}L\right), \\ \lambda_3 &= -\exp\left(\frac{L}{L_b}\right) \left(\frac{C_S + E_S}{L_b} + S_S k_{M2}\right), \\ \lambda_4 &= -S_S \sinh(-k_{M2}L) - C_S \cosh(-k_{M2}L) - E_S, \end{aligned}$$

the two boundary conditions reduce to the system

$$K_1 \lambda_1 + K_2 \lambda_2 = \lambda_3, \quad (86a)$$

$$K_1 + K_2 = \lambda_4. \quad (86b)$$

This system has for solution

$$\begin{aligned} K_1 &= \frac{\lambda_3 - \lambda_2 \lambda_4}{\lambda_1 - \lambda_2} \\ K_2 &= \frac{\lambda_3 - \lambda_1 \lambda_4}{\lambda_2 - \lambda_1} \end{aligned}$$

A1.3 Derivatives of the leading order solutions

The first order solutions depend on the leading order solutions and its derivatives. The leading order solutions are already given in the main body of this document (see Eqs (61a) and (61b)). Some additional derivatives are

$$\frac{\partial u_0}{\partial z} = \frac{g}{i\sigma} \alpha_{m_2} r_{m_2} \sinh(r_{m_2} z) \quad (87a)$$

$$\frac{\partial^2 u_0}{\partial z^2} = \frac{g}{i\sigma} \alpha_{m_2} r_{m_2}^2 \cosh(r_{m_2} z) \quad (87b)$$

$$\frac{\partial \zeta_{02}}{\partial x} = C_{m_2} \exp\left(\frac{x}{2L_b}\right) \left(-\frac{1}{2L_b} + \frac{k_{m_2}^2 L_b}{2}\right) \sinh\left(\frac{k_{m_2}}{2}(x-L)\right), \quad (87c)$$

$$\begin{aligned} \frac{\partial^2 \zeta_{02}}{\partial x^2} = & C_{m_2} \exp\left(\frac{x}{2L_b}\right) \\ & \left(\left(-\frac{1}{4L_b^2} + \frac{k_{m_2}^2}{4}\right) \sinh\left(\frac{k_{m_2}}{2}(x-L)\right) + \left(-\frac{k_{m_2}}{4L_b} + \frac{L_b k_{m_2}^3}{4}\right) \cosh\left(\frac{k_{m_2}}{2}(x-L)\right) \right) \end{aligned} \quad (87d)$$

$$\begin{aligned} \zeta_{02}^2 = & \frac{C_{m_2}^2}{2} \exp\left(\frac{x}{L_b}\right) \\ & \left((L_b k_{m_2})^2 - 1 + (1 + k_{m_2}^2 L_b^2) \cosh(k_{m_2}(x-L)) - 2L_b k_{m_2} \sinh(k_{m_2}(x-L)) \right) \\ \left(\frac{\partial \zeta_{02}}{\partial x}\right)^2 = & C_{m_2}^2 \exp\left(\frac{x}{L_b}\right) \left(\left(\frac{L_b^2 k_{m_2}^4}{8} - \frac{k_{m_2}^2}{4} + \frac{1}{8L_b^2}\right) \cosh(k_{m_2}(x-L)) - \left(\frac{L_b^2 k_{m_2}^4}{8} - \frac{k_{m_2}^2}{4} + \frac{1}{8L_b^2}\right) \right) \end{aligned} \quad (87e)$$

$$\begin{aligned} \zeta_{02} \frac{\partial \zeta_{02}}{\partial x} = & C_{m_2}^2 \exp\left(\frac{x}{L_b}\right) \\ & \left(\left(-\frac{1}{4L_b} + \frac{k_{m_2}^2 L_b}{4}\right) + \left(\frac{1}{4L_b} - \frac{k_{m_2}^2 L_b}{4}\right) \cosh(k_{m_2}(x-L)) \right. \\ & \left. + \left(-\frac{k_{m_2}}{4} \frac{k_{m_2}^3 L_b^2}{4}\right) \sinh(k_{m_2}(x-L)) \right) \end{aligned} \quad (87g)$$

$$\begin{aligned} \zeta_{02} \frac{\partial^2 \zeta_{02}}{\partial x^2} = & C_{m_2}^2 \exp\left(\frac{x}{L_b}\right) \\ & \left(\left(-\frac{k_{m_2}^2}{4} + \frac{L_b^2 k_{m_2}^4}{8} + \frac{1}{8L_b^2}\right) \cosh(k_{m_2}(x-L)) - \frac{1}{8L_b^2} + \frac{L_b^2 k_{m_2}^4}{8} \right) \end{aligned} \quad (87h)$$

$$(87i)$$

and

$$\begin{aligned} \zeta_{02} \frac{\partial^2 \zeta_{02}}{\partial x^2} + \left(\frac{\partial \zeta_{02}}{\partial x}\right)^2 - \frac{1}{L_b} \zeta_{02} \frac{\partial \zeta_{02}}{\partial x} = & C_{m_2}^2 \exp\left(\frac{x}{L_b}\right) \left(\left(-\frac{k_{m_2}^2}{4} + \frac{k_{m_2}^4 L_b^2}{4}\right) \cosh(k_{m_2}(x-L)) \right. \\ & \left. + \left(-\frac{L_b k_{m_2}^3}{4} + \frac{k_{m_2}}{4L_b}\right) \sinh(k_{m_2}(x-L)) \right) \end{aligned} \quad (88a)$$

DEPARTMENT **MOBILITY & PUBLIC WORKS**
Flanders hydraulics Research

Berchemlei 115, 2140 Antwerp

T +32 (0)3 224 60 35

F +32 (0)3 224 60 36

waterbouwkundiglabo@vlaanderen.be

www.flandershydraulicsresearch.be